Supplementary Information (SI) for ChemComm.

Supporting Information (SI)

Distinct Roles of Te and Mo in Modulating the Activity and Selectivity of CO_2 Hydrogenation to Ethanol over CoFe catalyst

Zihan Zhao[a], Yan Shao[b], Zongliang Kou*[ac] and Huanhao Chen*[ac]

[a]*State Key Laboratory of Materials-Oriented Chemical Engineering, College of Chemical Engineering, Nanjing Tech University, Nanjing 211816, China*
[b]*School of Environmental Science and Engineering, Nanjing Tech University, Nanjing, 211816, PR China*
[c]*Quzhou Menbrane material innovation institute, Quzhou, 324000, China*

*Corresponding authors' e-mail: UniqueKZL@163.com (Z.K.); h.chen@njtech.edu.cn (H.C.)

Methods

Synthesis of catalysts

All chemical reagents were of analytical grade and used as received without further purification. Ultrapure water was used throughout all experimental procedures.

In a typical synthesis, an aqueous precursor solution was prepared by dissolving $Co(NO_3)_2{\cdot}6H_2O$ (1.02 g, Sigma-Aldrich, ≥99.99%) and $Fe(NO_3)_3{\cdot}9H_2O$ (5.79g, Sigma-Aldrich, ≥99.99%) in 100 mL of deionized water. Under continuous stirring, an alkaline precipitating agent—consisting of a 1:1 mass ratio of Na_2CO_3 to NaOH—was added dropwise to the metal salt solution while maintaining the pH at 9. The resulting suspension was aged at 80 °C for 30 min. The solid product was collected by high-pressure filtration, thoroughly washed with deionized water (1 L), and dried at 80 °C. The obtained precursor was then calcined at 500 °C for 4 h in static air. A series of cobalt-iron oxides with varying Co/Fe mass ratios were synthesized following the co-precipitation procedure described above. For clarity, the baseline catalyst with a cobalt-to-iron mass ratio of 1:4 is hereafter denoted as CoFe.

Mo- or Te-modified catalysts were prepared via an incipient wetness impregnation method. Typically, a calculated volume of an aqueous solution of molybdenum nitrate or tellurium nitrate was added dropwise to the as-prepared CoFe support. The mixture was stirred continuously for 12 h at room temperature and subsequently dried at 80 °C overnight to remove the solvent completely. The resulting solid was finally calcined at 500 °C for 4 h in static air. The obtained catalysts with different loadings are labeled as xM-CoFe, where M represents the dopant element (Mo or Te) and x denotes its nominal mass percentage (x = 0.5, 1, 1.5, or 2). For example, a catalyst impregnated with a solution corresponding to 0.5 wt% Te is designated as 0.5Te-CoFe.

Catalyst evaluation

The CO_2 hydrogenation performance was evaluated in a custom-built fixed-bed reactor constructed from stainless steel (6 mm internal diameter × 485 mm length). For each test, the catalytic bed was prepared by thoroughly mixing the pelletized catalyst (200 mg, sieved to 250-425 μm) with quartz sand (1 g, of matched particle size) to ensure uniform flow distribution and temperature profile within the isothermal zone of the reactor. Prior to the reaction, the catalyst was activated via *in situ* reduction under pure H_2 flow (50 mL min^{-1}) at 350 °C for 1 h. After reduction, the reactor temperature was adjusted to the target reaction temperature of 260 °C under N_2 flow. The reactant gas mixture ($H_2/CO_2/N_2$ = 3:1:1 molar ratio) was then introduced at a total flow rate of 20 mL min^{-1}, corresponding to a gas hourly space velocity (GHSV) of 6,000 mL g_{cat}^{-1} h^{-1}. The system pressure was subsequently raised to 5 MPa using a back-pressure regulator.

To prevent condensation of heavy products, all downstream transfer lines were maintained at 130 °C with digitally controlled heating tape. The effluent gas composition was analyzed online using an Agilent 8860 gas chromatograph equipped with an HP-PLOT/Q column and both FID and TCD detectors. Data were collected continuously until reaction steady state was reached, which was confirmed by stable product composition over time. Carbon balances during steady-state operation ranged between 98% and 102%. Key performance metrics-including CO_2 conversion (X_{CO_2}, %), product selectivity (S_i, %) and space-time yield of product (STY_i, g_i kg_{cat}^{-1} h^{-1}) were calculated according to Equations 1–3 provided below.

$$X_{CO_2} = \frac{F_{CO_2,in} - F_{CO_2,out}}{F_{CO_2,in}} \times 100 \tag{1}$$

$$S_i\,(\%) = \frac{F_{i,out}}{\sum F_{i,out}} \times 100 \tag{2}$$

$$STY_i\ (g_i\ kg_{cat}^{-1}\ h^{-1}) = \frac{F_{CO_2,in} \times X_{CO_2} \times S_i \times M_i \times 3600}{m_{cat}} \times 100 \tag{3}$$

where F (mol s^{-1}) denotes the molar flow rate of reactants and products, m_{cat} (g) is the weight of the catalyst, and M_{EtOH}(46 g mol^{-1}) is the molar mass of Ethanol.

Characterizations. The chemical composition and structural properties of the synthesized CoFe, 0.5Mo-CoFe, and 0.5Te-CoFe catalysts were systematically characterized using a suite of analytical techniques. The actual metal loadings of Co, Fe, Mo, and Te in the catalysts were determined by Inductively Coupled Plasma-Optical Emission Spectroscopy (ICP-OES, Agilent 720). Morphological and elemental distribution analyses were performed using High-Resolution Transmission Electron Microscopy (HRTEM), High-Angle Annular Dark-Field Scanning TEM (HAADF-STEM), and Energy-Dispersive X-ray Spectroscopy (EDS) mapping. These analyses were conducted on a JEOL JEM-2100F electron microscope operating at 200 kV, equipped with both HAADF and Super-X EDS detectors. Further atomic-resolution HAADF-STEM imaging and EDS mapping of the reduced catalysts were obtained using a Thermo Fisher Scientific Titan G2 microscope, also operating at 200 kV.

X-ray Photoelectron Spectroscopy (XPS). The surface chemical states of the catalysts were investigated by X-ray Photoelectron Spectroscopy (XPS) on a Thermo Fisher ESCALAB 250XI spectrometer. All binding energies were calibrated relative to the C 1s peak at 284.8 eV. For the reduced samples, *in situ* pre-reduction treatment was carried out at 350 °C under a pure H_2 flow (50 mL min^{-1}) in a pretreatment chamber connected to the XPS analysis chamber, ensuring no exposure to air before measurement.

X-ray Absorption Fine Structure (XAFS). The local coordination environment and electronic structure of the Co and Fe atoms were probed by static X-ray Absorption Fine Structure (XAFS) spectroscopy at the Co *K*-edge and Fe *K*-edge. Measurements were conducted on a laboratory-based XAFS spectrometer (Rapid XAFS 2M, Anhui Absorption Spectroscopy Analysis Instrument Co., Ltd.) using a Mo target X-ray source operated at 20 kV and 20 mA. A Si (553) spherically bent crystal analyzer (SBCA) with a 500 mm radius of curvature was used as the monochromator. The XAFS data were collected in transmission mode using a silicon drift detector (SDD). The energy calibration for each measurement was performed using a corresponding Co or Fe metal foil, and all data were collected within a single, continuous period to ensure consistency.

H_2-TPR measurements. Reduction behaviors and surface adsorption properties were evaluated by chemisorption measurements on a BELCAT II instrument equipped with a Thermal Conductivity Detector (TCD). For H_2 Temperature-Programmed Reduction (H_2-TPR), approximately 30 mg of catalyst was pretreated in an Ar flow at 350 °C for 1 h to remove surface contaminants. The TPR profile was then recorded from 50 to 850 °C under a 10 vol% H_2/Ar flow at a heating rate of 10 °C min^{-1}.

CO_2 Temperature-Programmed Desorption (CO_2-TPD). Approximately 30 mg sample was first reduced *in situ* in a 10 vol% H_2/Ar flow at 350 °C for 1 h. After cooling to 60 °C under He, the catalyst was saturated with a 10 vol% CO_2/He flow for 1 h. Physically adsorbed CO_2 was then removed by purging with He, followed by programmed desorption from 60 to 850 °C in a He flow.

CO Temperature-Programmed Desorption (CO-TPD). Approximately 30 mg sample was first reduced *in situ* in a 10 vol% H_2/Ar flow at 350 °C for 1 h. After cooling to 60 °C under He, the catalyst was saturated with a 10 vol% CO/He flow for 1 h. Physically adsorbed CO was then removed by purging with He, followed by programmed desorption from 60 to 850 °C in a He flow.

Diffuse Reflectance Infrared Fourier Transform Spectroscopy (DRIFTS) using CO as a probe molecule (CO-DRIFTS). Experiments were performed on a Thermo Scientific Nicolet iS50 FTIR spectrometer equipped with a Harrick DRIFTS cell and a liquid N_2-cooled Mercury Cadmium Telluride (MCT) detector. Prior to measurement, catalysts were reduced *in situ* in H_2 flow at 350 °C for 1 h. After reduction, the system was cooled to 50 °C under Ar to collect a background spectrum. The catalysts were then exposed to a 2 vol% CO/Ar flow (50 mL min^{-1}) at 50 °C and atmospheric pressure for 60 min. Subsequently, the gas phase and weakly adsorbed CO were removed by purging with pure Ar for an additional 60 min, while the DRIFTS spectra were continuously collected by averaging 64 scans at a resolution of 8 cm^{-1}.

***In situ* Diffuse Reflectance Infrared Fourier Transform Spectroscopy (DRIFTS) using CO_2 as a probe molecule (CO_2-DRIFTS).** Experiments were performed on a Thermo Scientific Nicolet iS50 FTIR spectrometer equipped with a Harrick DRIFTS cell and a liquid N_2-cooled Mercury Cadmium Telluride (MCT) detector. Prior to measurement, catalysts were reduced *in situ* in H_2 flow at 350 °C for 1 h. Subsequently, the temperature was lowered to 260 °C to collect a background spectrum. *In situ* DRIFTS experiments were then performed at 3 MPa according to the following procedure: the catalysts were exposed to a reaction mixture of 10 vol% CO_2 (balanced with Ar) at a total flow rate of 50 mL min^{-1} and 260 °C for 60 min. Subsequently, the gas phase and weakly adsorbed CO_2 were removed by purging with pure Ar for an additional 60 min, during which time the DRIFTS spectra were continuously collected by averaging 64 scans at a resolution of 8 cm^{-1}.

***In situ* DRIFTS spectra of the CO_2+H_2 reaction.** High-pressure *in situ* diffuse reflectance infrared Fourier transform spectroscopy (DRIFTS) coupled with mass spectrometry (MS) was further employed to investigate the surface reaction mechanisms of CO_2 hydrogenation over the developed catalysts. The experiments were conducted using a Thermo Scientific Nicolet iS50 FTIR spectrometer equipped with a Harrick Scientific DRIFTS cell and a liquid N_2-cooled mercury cadmium telluride (MCT) detector, which was connected online to online mass spectrometer (Hidden QGA). Prior to each experiment, all catalysts were pre-reduced in a flow of 10 vol% H_2/Ar at 350 °C for approximately 1 h. Subsequently, the temperature was lowered to 260 °C to collect a background spectrum. *In situ* DRIFTS experiments were then performed at 3 MPa according to the following procedure: the catalysts were exposed to a reaction mixture of 10 vol% CO_2 and 30 vol% H_2 (balanced with Ar) at a total flow rate of 50 mL min^{-1} and 260 °C for 90 min. DRIFT spectra were recorded *in situ* by averaging 64 scans at a resolution of 8 cm^{-1}. Throughout the measurements, the composition of the effluent gas was monitored in real time by MS. The monitored mass-to-charge (m/z) signals included H_2 (m/z = 2), CO_2 (m/z = 44), CO (m/z = 28), CH_4 (m/z = 16), CH_3OH (m/z = 32), and C_2H_5OH (m/z = 46). This combined DRIFTS-MS approach enables the simultaneous observation of surface intermediates and gaseous products, thereby providing insights into the reaction pathways and kinetic behavior during CO_2 hydrogenation.

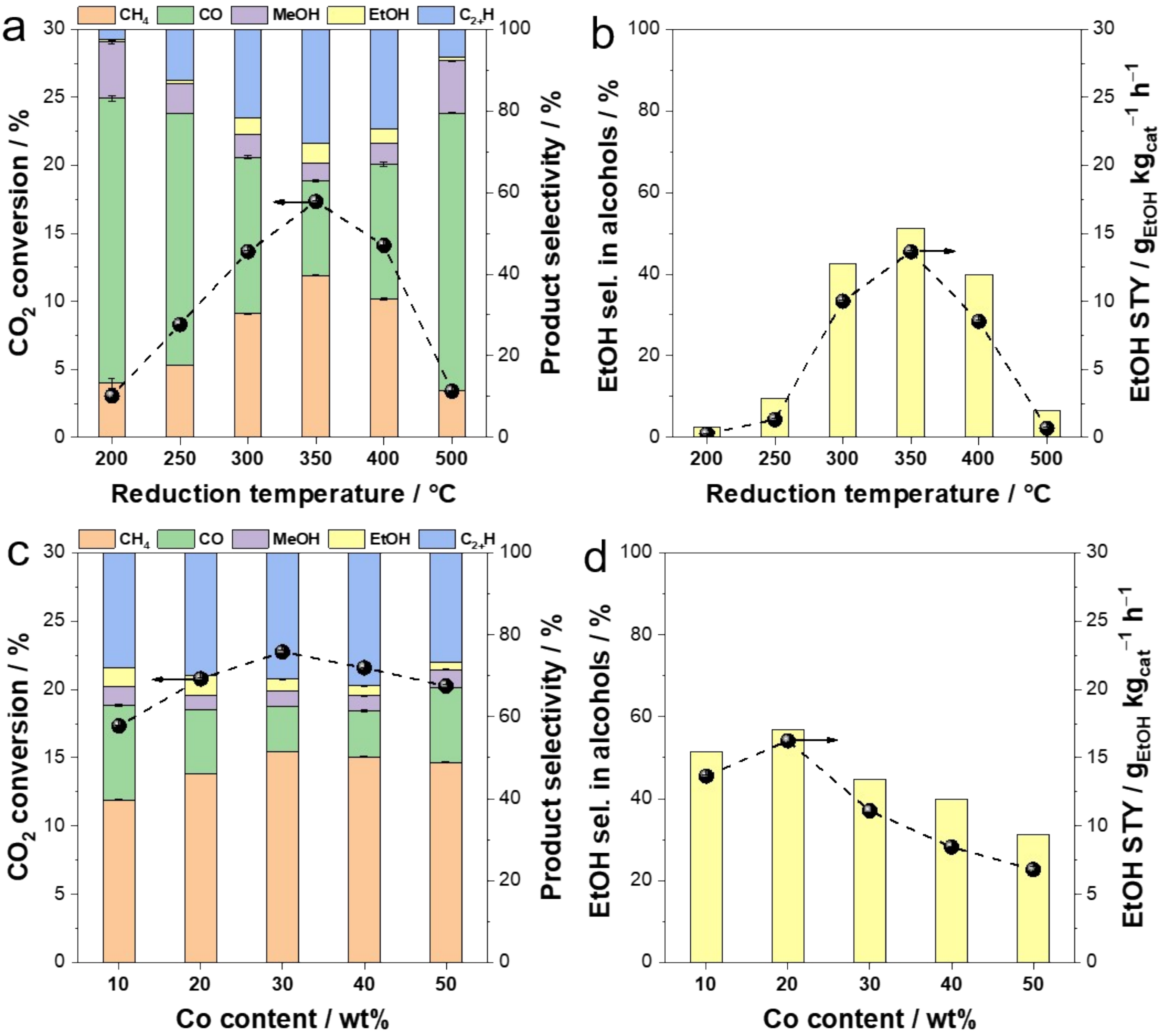

Figure S1. Catalytic performance of CO_2 hydrogenation over CoFe catalysts. (a, b) effect of Co content: (a) CO_2 conversion and product selectivity; (b) alcohols selectivity in liquid products and corresponding ethanol STY. (c, d) effect of reduction temperature: (c) CO_2 conversion and product selectivity; (d) alcohols selectivity in liquid products and corresponding ethanol STY. (Experimental conditions: T = 300 °C, P = 5.0 MPa, $H_2/CO_2/N_2$ = 3:1:1, and GHSV=6000 mL g_{cat}^{-1} h^{-1}).

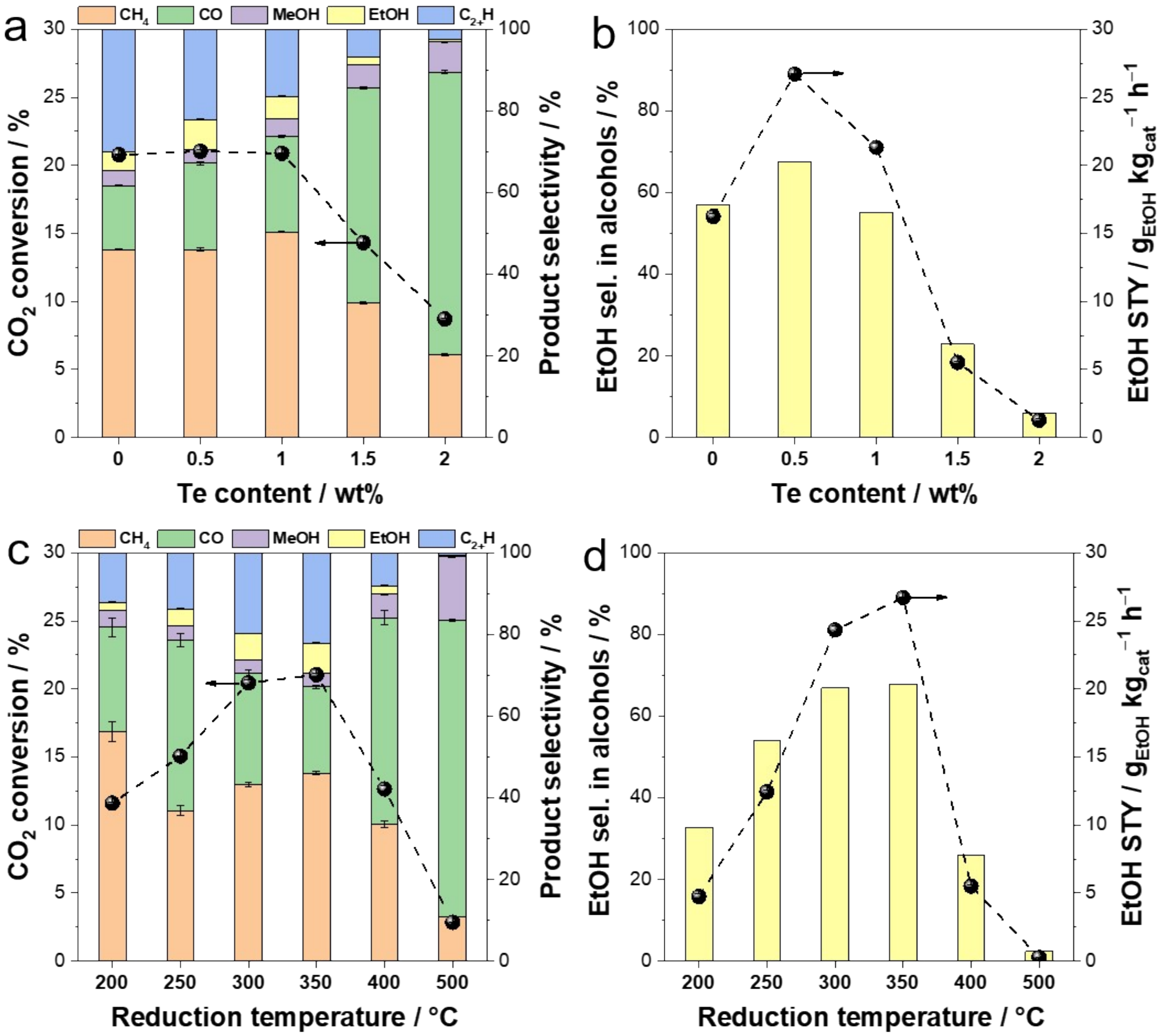

Figure S2. Catalytic performance of CO_2 hydrogenation over Te-CoFe catalysts. (a, b) effect of Co content: (a) CO_2 conversion and product selectivity; (b) alcohols selectivity in liquid products and corresponding ethanol STY. (c, d) effect of reduction temperature: (c) CO_2 conversion and product selectivity; (d) alcohols selectivity in liquid products and corresponding ethanol STY. (Experimental conditions: T = 300 °C, P = 5.0 MPa, $H_2/CO_2/N_2$ = 3:1:1, and GHSV=6000 mL g_{cat}^{-1} h^{-1}).

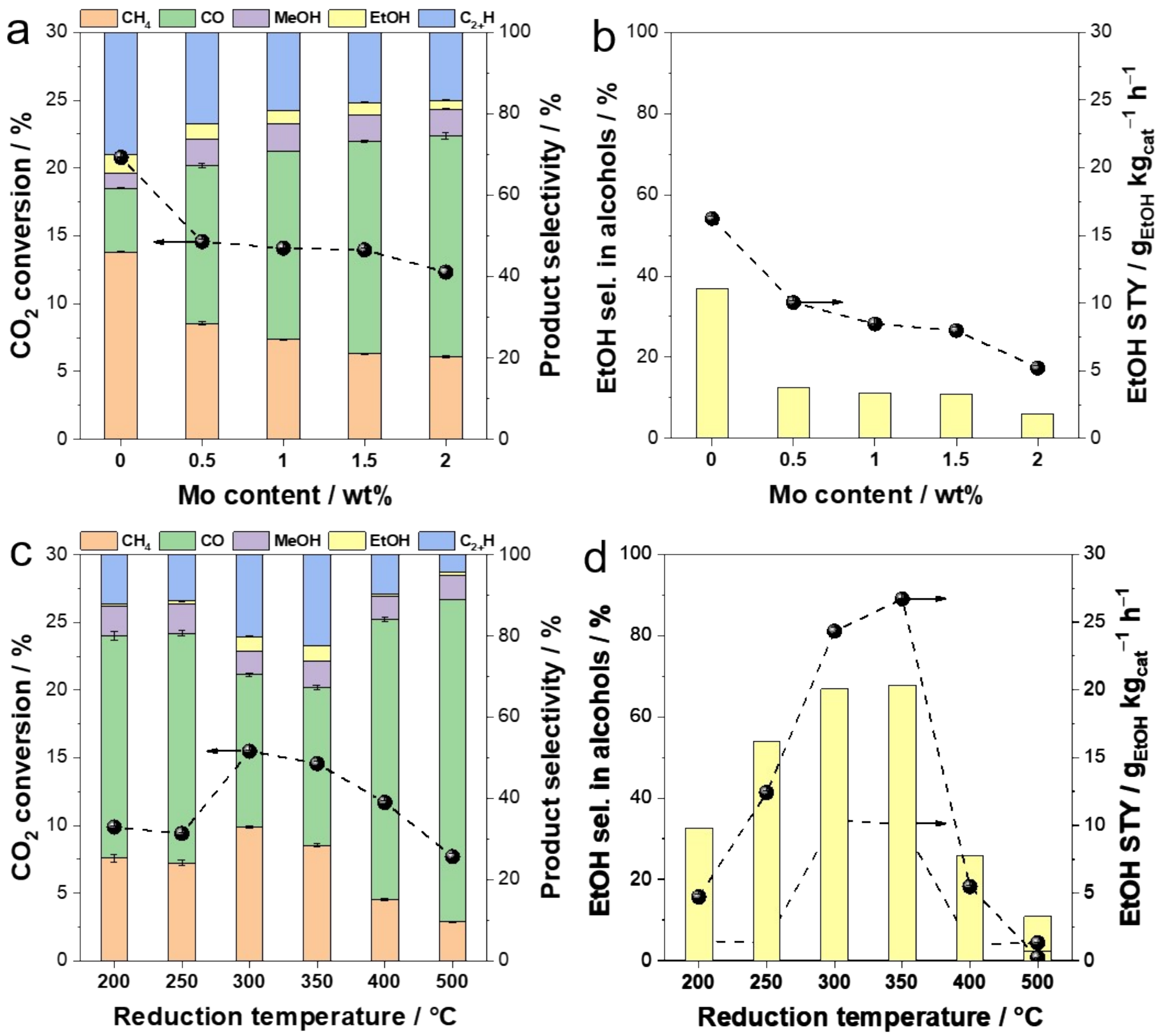

Figure S3. Catalytic performance of CO_2 hydrogenation over Te-CoFe catalysts. (a, b) effect of Co content: (a) CO_2 conversion and product selectivity; (b) alcohols selectivity in liquid products and corresponding ethanol STY. (c, d) effect of reduction temperature: (c) CO_2 conversion and product selectivity; (d) alcohols selectivity in liquid products and corresponding ethanol STY. (Experimental conditions: T = 300 °C, P = 5.0 MPa, $H_2/CO_2/N_2$ = 3:1:1, and GHSV=6000 mL g_{cat}^{-1} h^{-1}).

Table S1. Comparison of higher alcohols synthesis activity from CO_2 hydrogenation over 0.5Te-CoFe catalyst with some advanced catalysts in the literature.

Catalyst	T (°C)	P (MPa)	GHSV (mL g_{cat}^{-1} h^{-1})	Selectivity (%)					X_{CO2} (%)	Ref
				CO	C_xH_y	ROH	ROH			
							C_1	C_2		
Na-Co/SiO_2	250	5	4000	29.1	61.4	9.5	33.0	62.8	18.8	[1]
Na-Fe_3O_4	320	3	8000	14.3	81.7	4.0	-	-	34.0	[2]
Fe-Co/K-Al_2O_3	340	2	9000	10.4	89.6	-	-	-	36.6	[3]
0.5MnFe	340	2	-	7.9	90.6	1.5	-	-	10.0	[4]
RhFe-SiO_2	260	5	-	19.7	34.7	45.6	64.8	35.2	26.7	[5]
$Na_1Mo_{12}Fe_{87}$	320	5	24000	63.2	20.1	16.7	79.6	20.4	10.7	[6]
2%Na-Co_2C/SiO_2	250	5	6000	26.3	61.2	12.5	13.2	60.6	21.5	[7]
Cs-CuFeZn	330	5	4500	20.7	54.2	21.0	6.0	45.0	36.6	[8]
CuNaFe	310	3	28800	17	65.2	~10	-	-	32.3	[9]
FeCuGaZn-0.75	340	5	6000	16.2	27.2	31.9	2.0	25.4	26.0	[10]
4.6K-CMZF	320	5	6000	31.2	51.6	17.2	10.3	77.3	30.4	[11]
0.5Te-CoFe	260	5	6000	21.2	68.0	10.8	32.4	67.6	21.0	This work
0.5Te-CoFe	280	5	6000	27.8	62.6	9.6	27.1	72.9	23.5	This work
0.5Te-CoFe	300	5	6000	29.6	62.8	7.6	22.5	77.5	25.5	This work
0.5Te-CoFe	320	5	6000	25.6	67.9	6.5	40.1	59.9	29.9	This work
0.5Te-CoFe	340	5	6000	20.1	77.1	2.8	43.2	56.8	35.8	This work

Table S2. Product distribution of a series of CoFe catalysts.

Catalyst	Selectivity (%)					X_{CO2}(%)
	CH_4	CO	CH_3OH	C_2H_5OH	$C_{2+}H$	
10CoFe	39.7	23.1	4.5	4.7	28.0	17.3
20CoFe	46.1	15.6	3.6	4.8	29.9	20.8
30CoFe	51.4	11.2	3.7	3.0	30.8	22.7
40CoFe	50.2	11.2	3.6	2.4	32.5	21.6
50CoFe	48.9	18.3	4.3	1.9	26.6	20.2
0.5Te-CoFe	46.0	21.2	3.5	7.3	22.0	21.0
1.0Te-CoFe	50.4	23.4	4.4	5.4	16.4	20.9
1.5Te-CoFe	32.9	52.8	5.7	1.7	6.9	14.3
2.0Te-CoFe	20.3	69.3	9.3	0.6	2.5	8.7
0.5Mo-CoFe	28.4	38.8	3.6	3.8	22.4	14.6
1.0Mo-CoFe	24.5	46.3	6.5	3.2	19.3	14.1
1.5Mo -CoFe	21.1	52.1	6.6	3.0	17.2	14.0
2.0Mo-CoFe	20.3	54.3	6.6	2.2	16.7	12.3

Table S3. ICP-OES analysis of the actual metal loading of fresh catalysts.

Catalyst	Metal loading (wt.%)			
	Co	Fe	Te	Mo
CoFe	11.3	44.2	-	-
0.5Te-CoFe	12.6	41.1	0.5	-
0.5Mo-CoFe	11.8	45.4	-	0.5

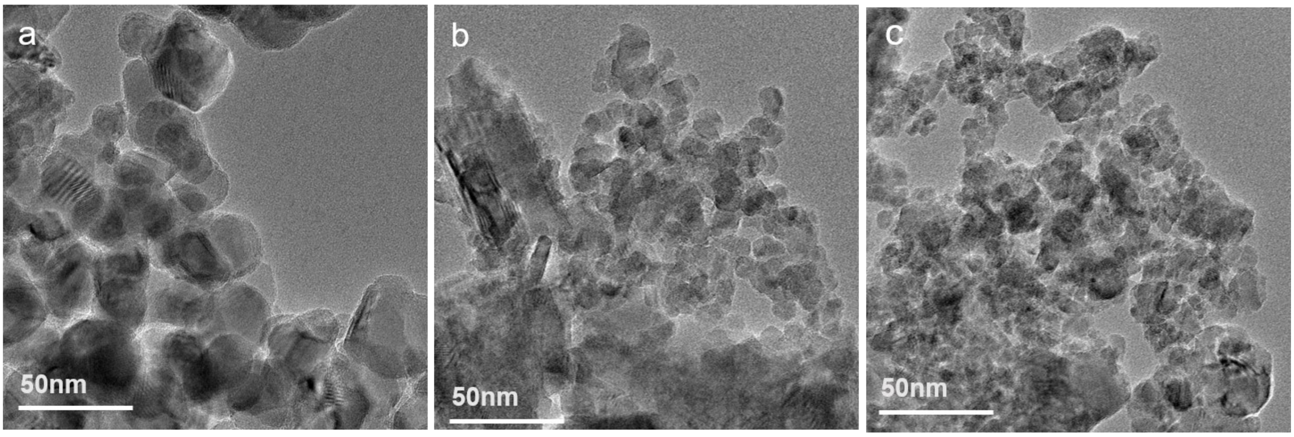

Figure S4. Low-magnification TEM images of the (a) 0.5Te-CoFe, (b) 0.5Mo-CoFe, and (c) CoFe catalysts.

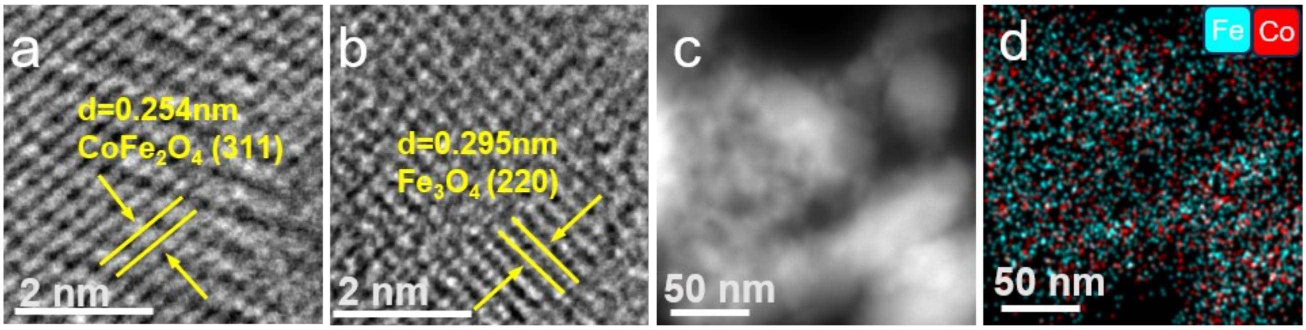

Figure S5. (a, b) HRTEM image, (c, d) HAADF and corresponding EDS mapping images of the CoFe catalyst.

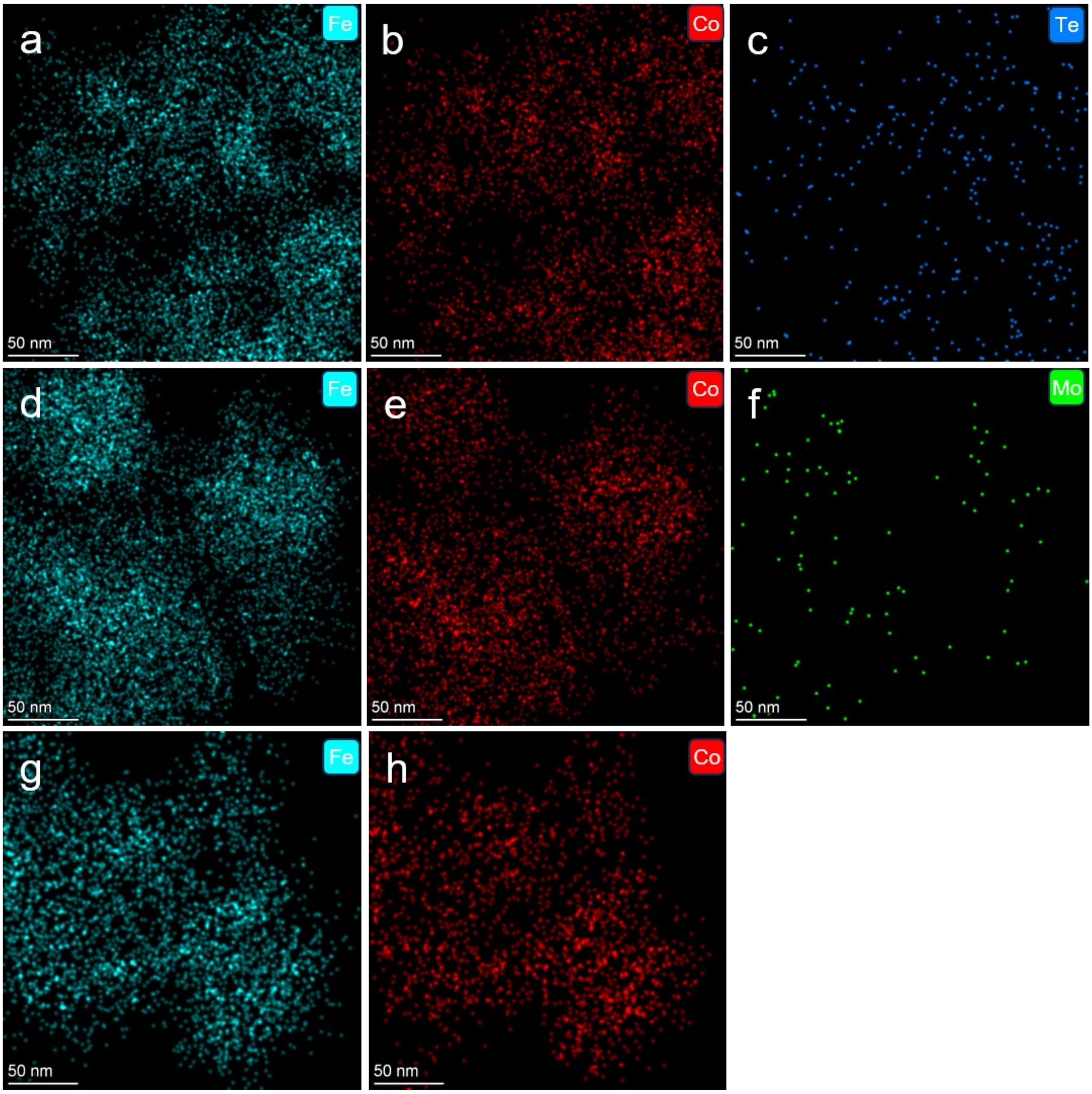

Figure S6. EDS-mapping spectra for (a-c) 0.5Te-CoFe, (d-f) 0.5Mo-CoFe and (g, h) CoFe catalyst.

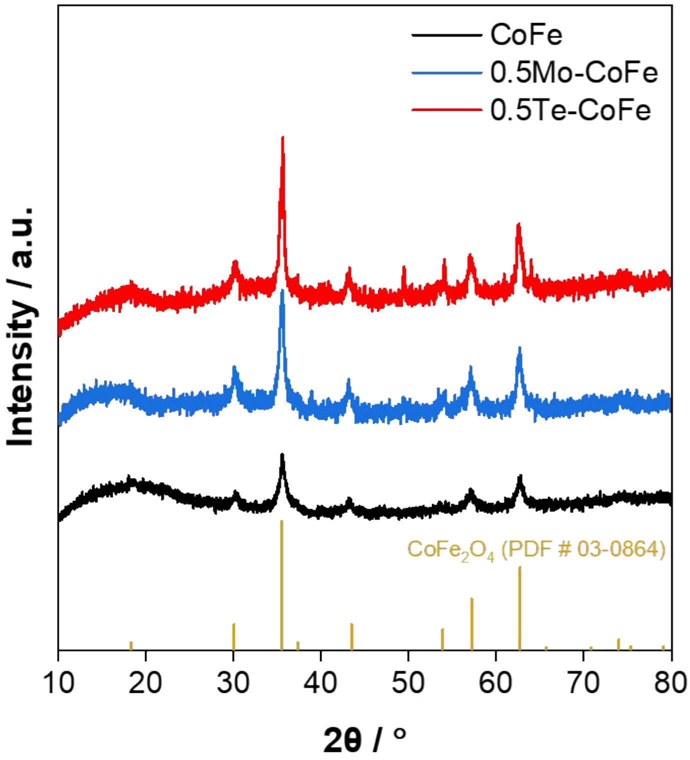

Figure S7. The XRD patterns of the CoFe, 0.5Te-CoFe and 0.5Mo-CoFe catalysts.

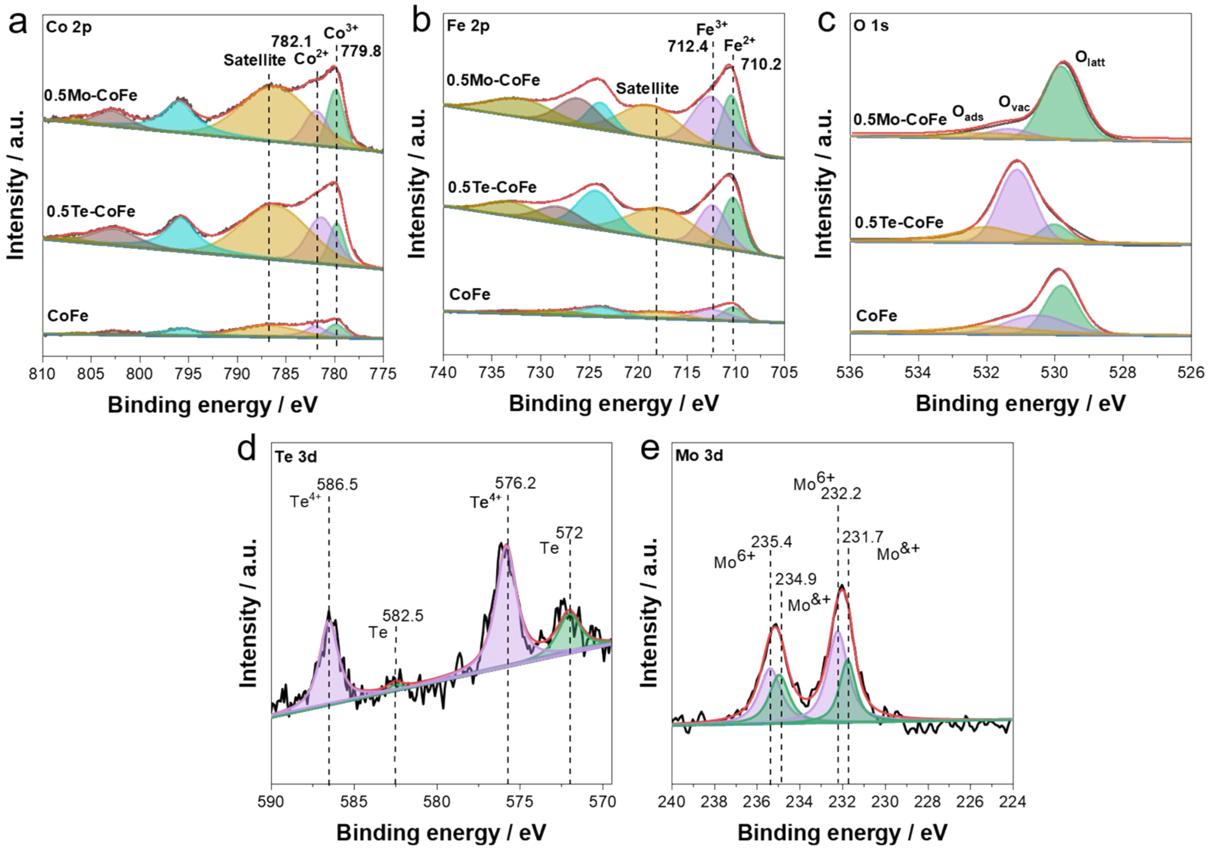

Figure S8. (a) Co 2p XPS spectra of reduced CoFe, 0.5Te-CoFe and 0.5Mo-CoFe catalysts, (b) Fe 2p XPS spectra of reduced CoFe, 0.5Te-CoFe and 0.5Mo-CoFe catalysts, (c) O 1s XPS spectra of reduced the catalysts (d) Te 3d XPS spectra of reduced 0.5Te-CoFe catalysts, (e) Mo 3d XPS spectra of reduced 0.5Mo-CoFe catalysts (Reduction conditions: 350 °C and 50 mL min^{-1} H_2 flow for 1 h).

Table S4. Co^{2+} and Co^{3+} intensity ratio in the Co 2p spectra of a series of CoFe Catalysts.

Catalyst	Co^{2+}	Co^{3+}	Co^{2+} / (Co^{2+}+Co^{3+})	Co^{3+} / (Co^{2+}+Co^{3+})
CoFe	19014.8	20243.2	0.49	0.51
0.5Te-CoFe	100444.6	45281.2	0.69	0.31
0.5Mo-CoFe	54925.9	79367.2	0.41	0.59

Table S5. Fe^{2+} and Fe^{3+} intensity ratio in the Fe 2p spectra of a series of CoFe Catalysts.

Catalyst	Fe^{2+}	Fe^{3+}	Fe^{2+} / (Fe^{2+}+Fe^{3+})	Fe^{3+} / (Fe^{2+}+Fe^{3+})
CoFe	50733.6	74155.6	0.41	0.59
0.5Te-CoFe	211268.8	214050.4	0.50	0.50
0.5Mo-CoFe	187882.6	336574.9	0.36	0.64

Table S6. O_{latt}, O_{vac} and O_{ads} intensity ratio in the O 1s spectra of a series of CoFe Catalysts.

Catalyst	O_{latt}	O_{vac}	O_{ads}	O_{latt}/ (O_{latt} + O_{vac} + O_{ads})	O_{vac}/ (O_{latt} + O_{vac} + O_{ads})	O_{ads}/ (O_{latt} + O_{vac} + O_{ads})
CoFe	217614.9	154830.7	132869.7	0.43	0.31	0.26
0.5Te-CoFe	73126.13	353256.3	201243.3	0.12	0.56	0.32
0.5Mo-CoFe	359713.4	57371.91	60303.92	0.75	0.12	0.13

Table S7. Surface atomic fraction of Te/Mo relative to total metals.

Catalyst	Promoter Te/Mo	Co	Fe	Surface atomic fraction (XPS, at%)	Bulk atomic fraction (ICP, at%)	Enrichment factor (surface/bulk)
0.5Te-CoFe	3136.7	145725.8	425319.2	0.54	0.48	1.13
0.5Mo-CoFe	3384.4	134211.3	524457.5	0.51	0.51	1.00

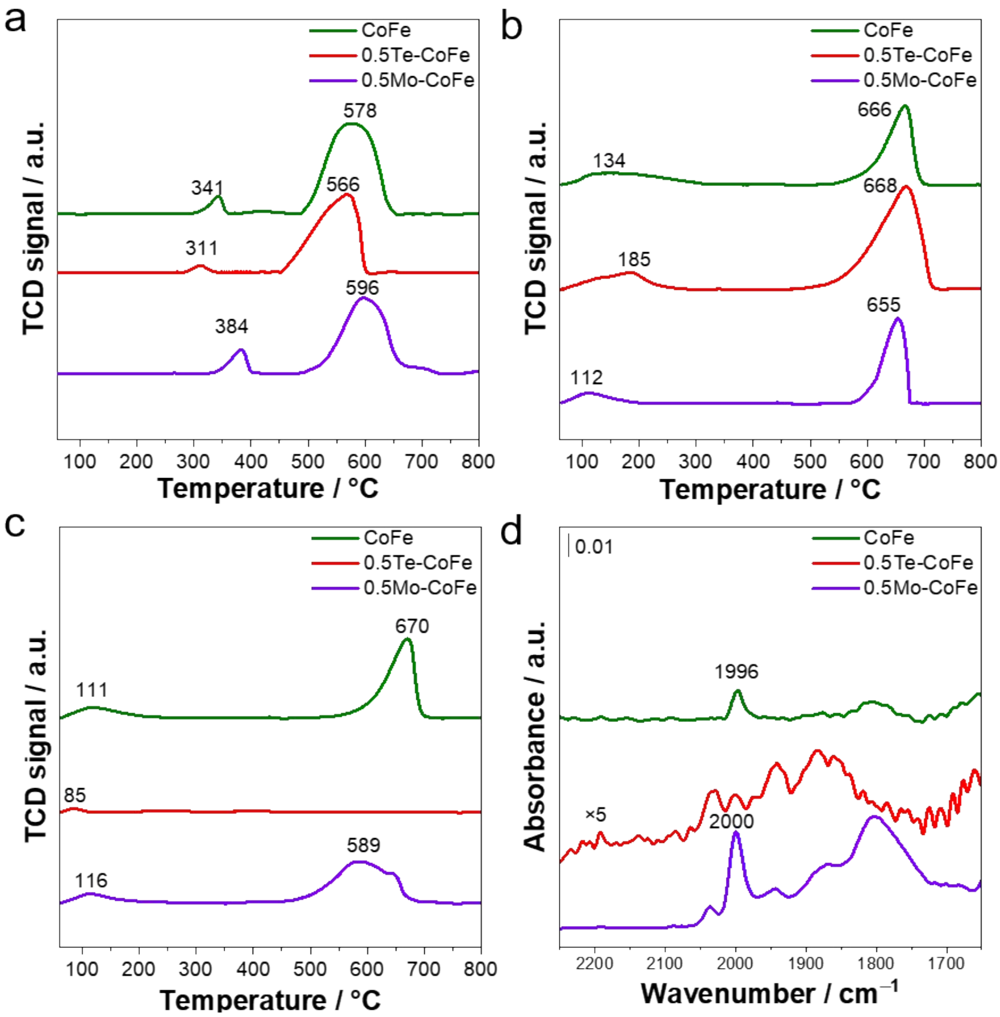

Figure S9. (a) H_2-TPR, (b) CO_2-TPD and (c) CO-TPD profiles of the catalysts and (d) *In situ* DRIFTS spectra of CO desorption profiles of the catalysts. (Reduction conditions: 350 °C and 50 mL min^{-1} H_2 flow for 1 h).

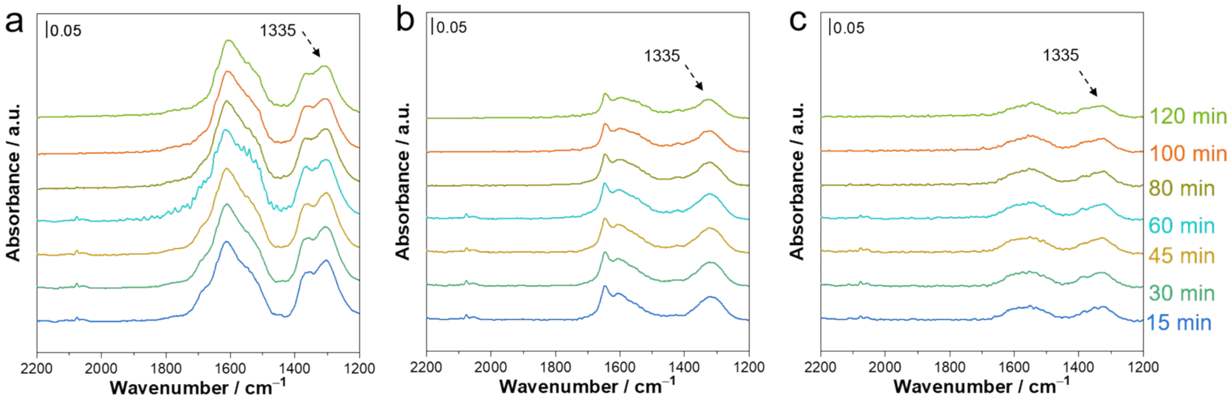

Figure S10. *In situ* CO_2 DRIFTS spectra of the catalysts. (a) 0.5Te-CoFe, (b) CoFe and (c) 0.5Mo-CoFe. (Reduction conditions: 350 °C and 50 mL min^{-1} H_2 flow for 1 h. Subsequently, the catalyst was exposed to CO_2 for 60 min, followed by switching to Ar for another 60 min).

Table S8. H_2 consumption amount of the prepared catalysts.

Catalyst	H_2 consumption amount / mmol g_{cat}^{-1}	H_2 consumption amount / mmol g_{cat}^{-1}
CoFe	0.02	0.34
0.5Te-CoFe	0.02	0.35
0.5Mo-CoFe	0.05	0.30

Table S9. CO_2 adsorption amount of the prepared catalysts.

Catalyst	Weak adsorption amount / mmol g_{cat}^{-1}	Strong adsorption amount / mmol g_{cat}^{-1}
CoFe	0.42	1.21
0.5Te-CoFe	0.40	1.46
0.5Mo-CoFe	0.18	1.11

Table S10. CO adsorption amount of the prepared catalysts.

Catalyst	CO adsorption amount / mmol g_{cat}^{-1}	CO adsorption amount / mmol g_{cat}^{-1}
CoFe	0.09	0.48
0.5Te-CoFe	0.12	0.03
0.5Mo-CoFe	0.06	0.55

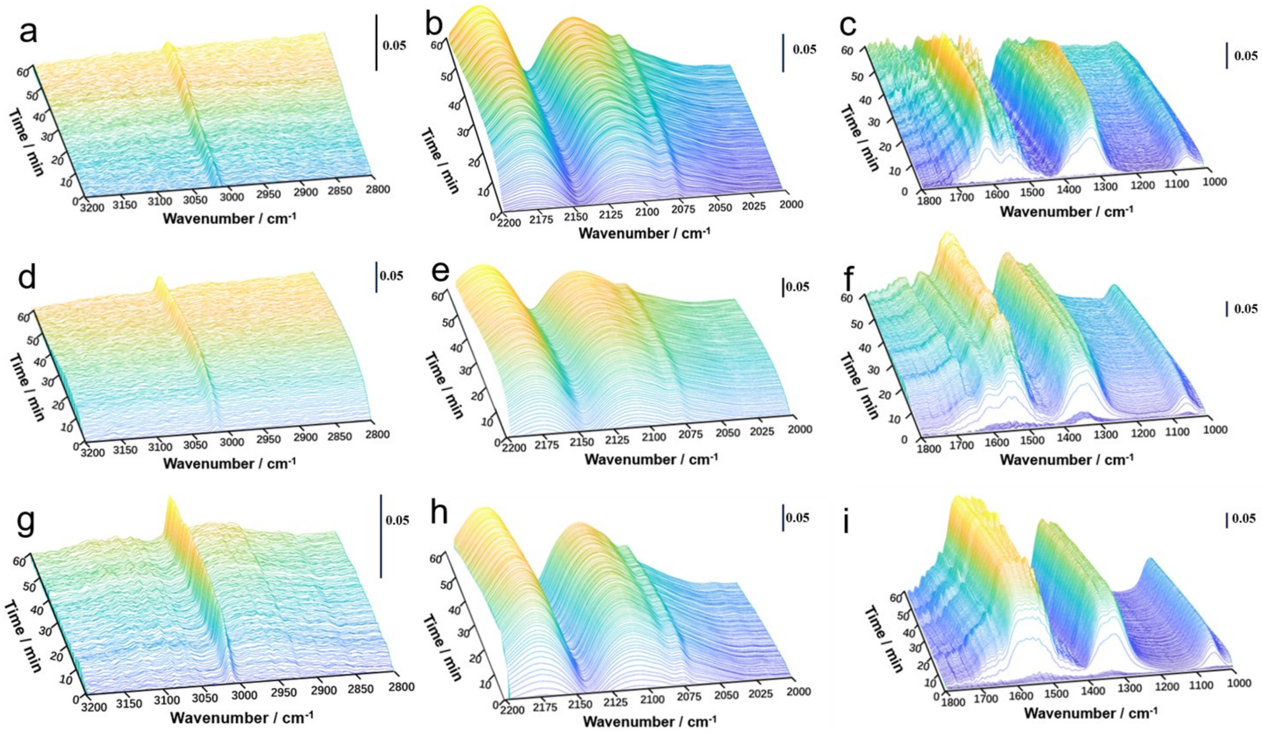

Figure S11. *In situ* DRIFTS spectra of (a-c) CoFe, (d-f) 0.5Mo-CoFe and (g-i) 0.5Te-CoFe under reaction condition for 60 minutes (Reduction conditions: 300 °C, 0.3 MPa, 10% H_2/Ar, 50 mL/min, 1h. Test condition: 300 °C, 3 MPa, 10% CO_2 / 10% Ar /30% H_2).

References

1. S. Zhang, X. Liu, Z. Shao, H. Wang and Y. Sun, *J. Catal.*, 2020, **382**, 86-96.
2. S. Kattel, P. Liu and J. G. Chen, *J. Am. Chem. Soc.*, 2017, **139**, 9739-9754.
3. T. Numpilai, N. Chanlek, Y. Poo-Arporn, C. K. Cheng, N. Siri-Nguan, T. Sornchamni, M. Chareonpanich, P. Kongkachuichay, N. Yigit, G. Rupprechter, J. Limtrakul and T. Witoon, *ChemCatChem.*, 2020, **12**, 3306-3320.
4. M. Al-Dossary, A. A. Ismail, J. L. G. Fierro, H. Bouzid and S. A. Al-Sayari, *Appl. Catal., B.*, 2015, **165**, 651-660.
5. D. Xu, Y. Wang, M. Ding, X. Hong, G. Liu and S. C. E. Tsang, *Chem.*, 2021, **7**, 849-881.
6. Y. Ge, A. J. Martín, M. Suvarna, T. Zou, F. Krumeich and J. Pérez-Ramírez, *Appl. Catal., B.*, 2025, **378**, 125578.
7. S. Zhang, Z. Wu, X. Liu, Z. Shao, L. Xia, L. Zhong, H. Wang and Y. Sun, *Appl. Catal., B.*, 2021, **293**, 120207.
8. D. Xu, M. Ding, X. Hong, G. Liu and S. C. E. Tsang, *ACS Catal.*, 2020, **10**, 5250-5260.
9. Z. Si, L. Wang, Y. Han, J. Yu, Q. Ge, C. Zeng and J. Sun, *ACS Sustainable Chem. Eng.*, 2022, **10**, 14972-14979.
10. Y. Ma, Y. Liu, Z. Huang, X. Han, L. Ye, X. Qin, H. Xu, L. Kong, J. Li and J. Zhang, *Sep. Purif. Technol.*, 2025, **364**, 132583.
11. D. Xu, M. Ding, X. Hong and G. Liu, *ACS Catal.*, 2020, **10**, 14516-14526.